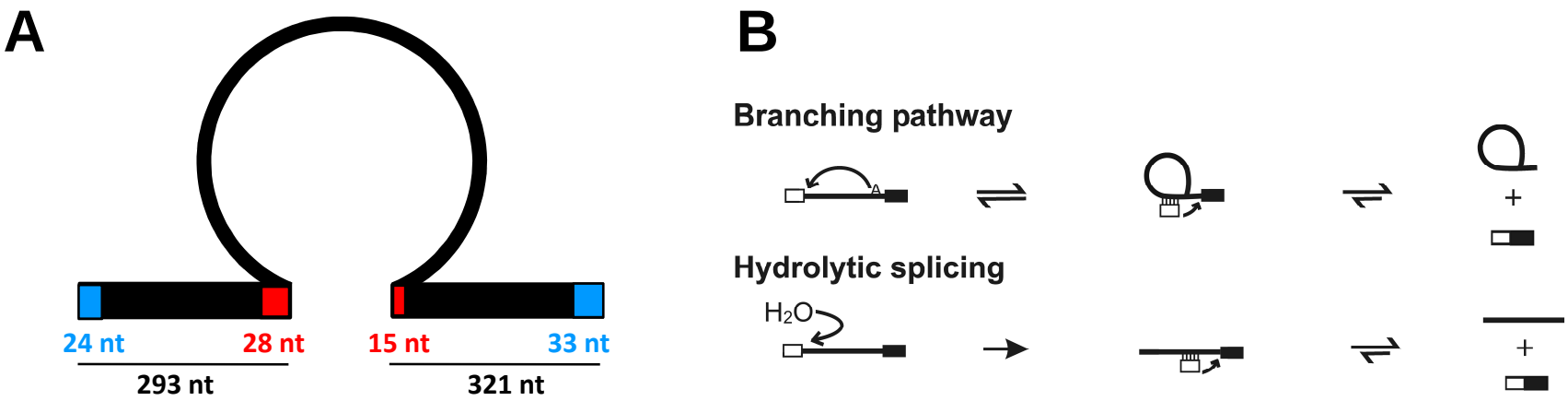

Supplementary Figure 1:

A: Schematic structure of splicing constructs used in this study.
The intron sequence is shown as a circle, the exons as bar. red: exons used in the SE construct; blue: vector-derived sequences in the long exon construct. Schematic not drawn to scale.
B: The branching and the hydrolytic pathway of group II intron splicing.
The intron is depicted as a line, the exons as white (5') and black (3') bars. The branchpoint adenosine is marked as A.

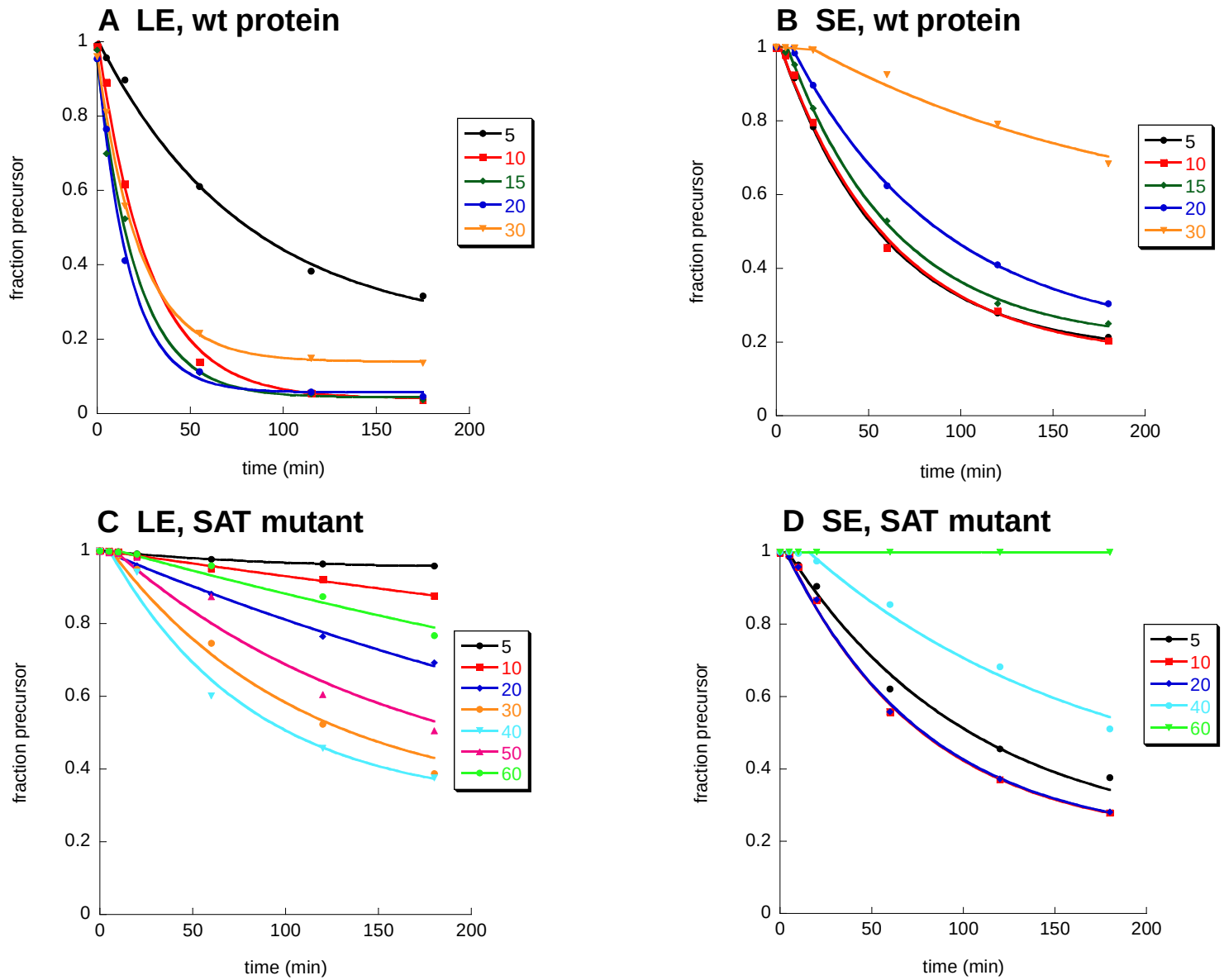

Supplementary Figure 2: Optimal Mss116 concentrations

A

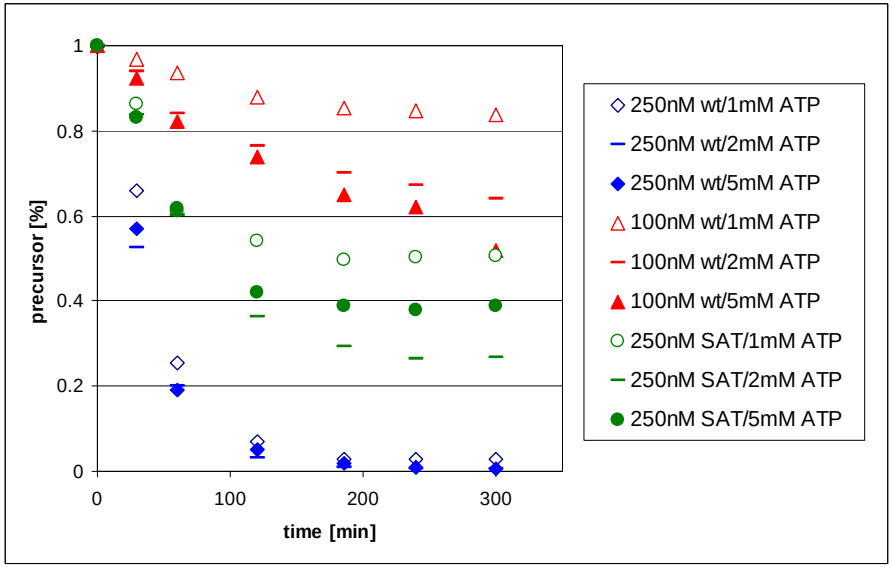

B

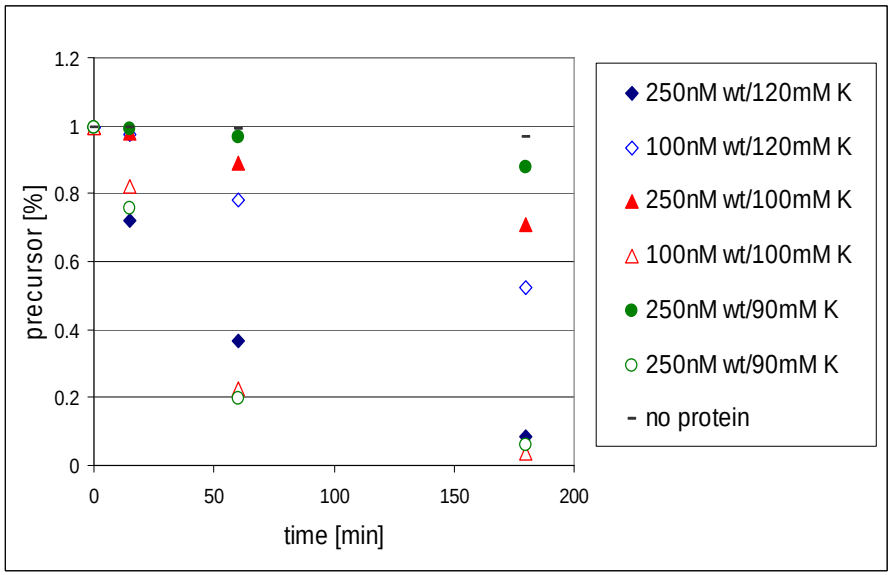

Supplementary Figure 3: Optimization of Cyt-19 mediated ai5γ splicing

A: Cyt-19-mediated LE splicing with varying ATP concentrations. While increasing the ATP concentration barely affects the reaction rate for 250 nM wild-type Cyt-19, it enhances splicing with 100 nM wild-type Cyt-19 and 250 nM of the Cyt-19 SAT mutant. The reaction with 250 nM wild-type Cyt-19 is probably so fast that it reaches completion before ATP becomes limiting. Note that these experiments were conducted using the conditions described in Solem et al. (i.e. 20nM RNA, 130 mM KCl)

B: LE splicing with 100 or 250 nM Cyt-19 and varying [K^+] concentrations. At 120 mM [K+], 250 nM Cyt-19 yields better splicing stimulation than 100 nM (blue diamonds), but at 100 or 90 mM [K+], 100 nM Cyt-19 is much more efficient than 250 nM (green circles, red triangles). Analogous experiments with SE suggest that at low [K^+], higher protein concentrations are even inhibitory, since they suppressed the background splicing of SE (data not shown). The Cyt-19 SAT/AAA mutant yielded similar results (data not shown).